Formation of the Hydrophobic Core of Ribonuclease A through Sequential Coordinated Conformational Transitions†

Ami Navon,[#,§] Varda Ittah,[#] Harold A. Scheraga,[*,‡] and Elisha Haas[#]

Faculty of Life Sciences, Bar Ilan University, Ramat Gan, Israel 52900, Department of Cell Biology, Harvard Medical School, 240 Longwood Avenue, Boston, Massachusetts 02115, and Baker Laboratory of Chemistry and Chemical Biology, Cornell University, Ithaca, New York 14853-1301

Received August 2, 2002; Revised Manuscript Received September 18, 2002

ABSTRACT: With steady-state and time-resolved fluorescence energy-transfer measurements, we determined the distributions of intramolecular distances in nine mutants to study the conformations of wild-type ribonuclease A in the reduced state under folding conditions. Although far-UV−CD measurements show no evidence for a secondary-structure transition, temperature- and GdnHCl-induced changes in intramolecular distance distributions in the reduced state revealed evidence for long-range subdomain structures in the denatured protein. These poorly defined structures, reflected here by wide distributions corresponding to a wide range of energies, form during refolding in a complex sequence of multiple subdomain transitions. A more well-defined structure emerges only when this structural framework, which directs the successive steps in the folding process, matures and is reinforced by stronger interactions such as disulfide bonds.

With a nonradiative excitation energy-transfer (TR-FRET)[1] technique, we previously showed that the C-terminal portion of bovine pancreatic ribonuclease A (RNase A) in the R_N state has interresidue distances that are closer to those of the native structure than to those of a statistical coil; i.e., the protein in the R_N state is poised to fold (*1*). Similar conclusions were deduced for other reduced−denatured proteins such as the bovine pancreatic trypsin inhibitor (*2*, *3*). In addition, the N-terminal portion of the RNase A chain in the R_N state is separated from the C-terminal core by larger intramolecular distances than in the native structure (1).

The reduced−denatured state of RNase A was the starting point for oxidative folding studies with dithiothreitol that led to a folding mechanism involving intermediate structures on several different pathways (*4*−*13*). Several of the intermediate folded structures were characterized; e.g., the structures of two three-disulfide intermediates were determined by multidimensional NMR spectroscopy (*14*, *15*), and a nonrandom distribution of one-disulfide bonds in the ensembles of intermediate species containing one (*16*), two (*17*), and three (*18*) disulfide bonds, respectively, was observed.

In this paper, we examine the starting material, viz., the reduced−denatured form of RNase A, and show that the R_N form can undergo (i) a thermal transition (and cold unfolding), indicated by changes of interresidue distance distributions, even though such transitions are not detected by circular dichroism, and (ii) several Gdn-HCl-induced conformational transitions, reflected in changes of interresidue distance distributions. These distributions of intramolecular distances (IDDs) between fluorescent probes were determined by TR-FRET measurements. For this purpose, nine pairs of sites in the RNase A molecule were labeled by a fluorescent donor (a genetically engineered tryptophan residue) and an acceptor probe (cysteines modified with 7-iodoacetamidocoumarin-4-carboxylic acid, I-Cca).

This paper focuses on the landscape of structures in the reduced−denatured form of RNase A before oxidative folding begins. Characterization of this form provides information about the starting state of protein folding models. In hierarchical folding models, it is assumed that secondary-structure elements form early in the folding process (*19*). Other studies show that the kinetics does not depend on secondary-structure formation, and that strong specific hydrophobic contacts seem to play a dominant role (*3*, *20*). One simulation (*21*) supports neither a pure hydrophobic collapse nor a diffusion−collision model, with folding beginning with formation of a few helical hydrogen bonds, followed later by a gradual concomitant formation of more hydrogen bonds, together with a reduction in the radius of gyration. It is currently unclear if the formation of secondary structure (native or non-native) is a general prerequisite for

† This work was supported by Grants GM-39372 and GM-24893 from the National Institutes of Health and by grants from the Israel Science Foundation, the U.S.-Israel Binational Science Foundation, and the Demedian Center for magnetic resonance research at Bar Ilan University. This work was also supported by the National Foundation for Cancer Research (U.S.A.).

* Correspondence should be addressed to H.A.S. E-mail: has5@cornell.edu.

[#] Bar Ilan University.

[§] Harvard Medical School.

[‡] Cornell University.

[1] Abbreviations: RNase A, bovine pancreatic ribonuclease A; R_N state, the reduced form of the protein in native buffer (i.e., under folding conditions); U state, the disulfide-intact protein denatured in 6 M GdnHCl; (*m*−*n*), designation of mutant, where *m* is the location of the tryptophan, and *n* is the location of a coumarin derivative; TR-FRET, time-resolved dynamic nonradiative excitation energy transfer; IDD, intramolecular distance distribution; DTT, dithiothreitol; GdnHCl, guanidinium hydrochloride; EDTA, ethylenediaminetetraacetic acid; TCEP, tris[2-carboxyethylphosphine]hydrochloride; HEPES, *N*-2-hydroxyethylpiperizine-*N*′-2-ethanesulfonic acid; I-Cca, 7-iodoacetamidocoumarin-4-carboxylic acid.

10.1021/bi020506p CCC: $22.00
Published on Web 11/09/2002

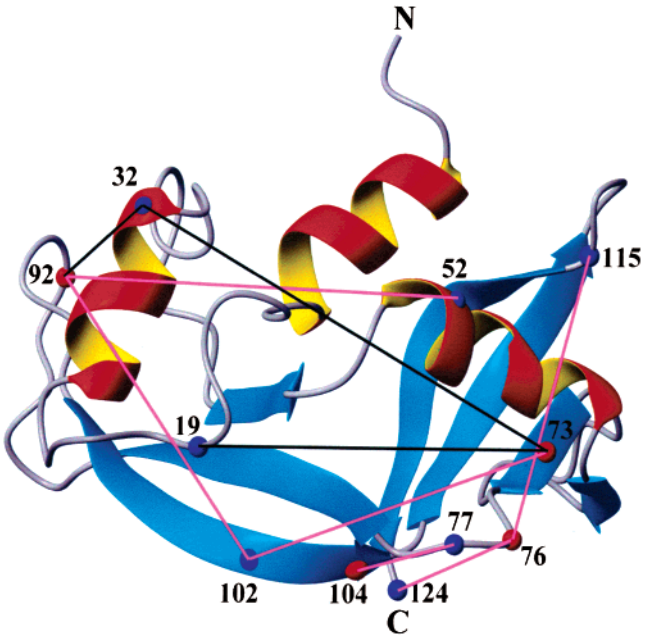

FIGURE 1: Ribbon diagram of bovine pancreatic ribonuclease A, taken from a high-resolution X-ray crystal structure (*22*), and showing the locations of the residues defining the segments whose conformational transitions were studied here. The α carbons of the four inserted tryptophan residues (the donors) are represented as red spheres. The α carbons of the seven non-native cysteine residues conjugated to coumarin (the acceptors) are represented by blue spheres. Nine colored straight lines designate the pairs of sites in specific segments. Black lines denote a segment involving both the N- and C-terminal parts of the molecule, and magenta lines denote segments in which both residues reside in the C-terminal part of the molecule.

the management of the folding transition. However, in a few cases it was shown that, even under drastic denaturing conditions where secondary-structure elements were unfolded, proteins showed native-like conformational preferences (*1*−*3*). It was suggested (*1*, *3*) that a few nonlocal interactions, which lead to the formation of long loops, can make a major contribution that populates weakly stabilized conformers, which are productive folding intermediates.

It is still an open question as to what determines the spatial location of the compaction nucleus. Characterization of the structure of the ensembles of conformations under partially folded conditions is expected to yield clues as to the type of interactions that direct the formation of compact structures and their transitions. Is there one global coordinated transition of all parts of the chain or a series of localized transitions? What is the role of local versus nonlocal interactions in the folding/unfolding transitions, and are the transitions within the hydrophobic core of reduced RNase A cooperative?

The determination of changes in selected distributions of long-range intramolecular distances by the FRET methods provides a procedure to obtain structural parameters, which are relevant to these issues. The temperature- and GdnHCl-induced conformational transitions monitored by steady-state and time-resolved FRET measurements reported here were designed to address these questions. The changes of intramolecular distance distributions in the set of nine pairs of site-specifically labeled RNase A mutants [Figure 1 (*22*)] in the reduced state (R_N) were monitored. The results obtained here show that, in reduced RNase A, which exhibits no evidence of secondary-structure content, structural elements associated with the C-terminal subdomain pass through a set of hierarchic transitions following the initial compaction transition.

MATERIALS AND METHODS

Preparation of the Different RNase A Species. The preparation of recombinant RNase A derivatives and mutants has been discussed in previous papers (*1*, *23*). In brief, a single tryptophan residue (at one of the positions 73, 76, 92, and 104) and a non-native cysteine residue (at one of the positions 19, 32, 52, 77, 102, 115, and 124), replacing the corresponding single solvent-exposed residue, were introduced into each mutant (Figure 1). The additional non-native cysteine was subsequently blocked by an alkylating fluorescent reagent (7-iodoacetamidocoumarin-4-carboxylic acid). These mutants are abbreviated *m*−*n*, where *m* is the location of the tryptophan and *n* is the location of a coumarin derivative on the additional cysteine. The labeled RNase A mutants were characterized by absorption and fluorescence spectroscopy, and the specificity of the labeling reactions with the fluorescent alkylating reagent was confirmed (*1*, *23*); their enzymatic activity was found to be similar to that of the native nonmodified RNase A (*1*). In six of these RNase A derivatives, the tryptophan−coumarin pairs spanned chain segments within the C-terminal hydrophobic core, viz., residues 73 to 124, and, in three of the derivatives**,** the tryptophan residue was located in the C-terminal portion of the chain while the coumarin was inserted in the N-terminal portion of the chain, viz., residues 1−60 (Figure 1). CD and fluorescence energy-transfer experiments were carried out on these derivatives as described previously (*1*, *23*).

Far-UV−CD Thermal Transition. Circular dichroism spectra were measured at various temperatures with a model 62A DS CD spectrometer (Aviv Associates, Lakewood, NJ), calibrated with a camphorsulfonic acid solution (*23*−*25*). Thermal transition measurements were made by varying the temperature from 20 to 80 °C in increments of 2 °C while monitoring the ellipticity at 220 nm. The temperatures were controlled within 0.1 °C. After reaching each target temperature, the solutions were allowed to equilibrate for 2 min. Prior to all spectroscopic measurements, the protein solutions were aspirated under vacuum, and their concentrations were measured spectrophotometrically. The raw CD measurements (in millidegrees) were converted to molar ellipticity [θ] and mean residue ellipticity $[\theta]_m$ (in deg·cm^2 dmol^{-1}) using molecular weight values computed from the amino acid composition.

Steady-State Fluorescence Measurements. Steady-state fluorescence measurements in the presence of different GdnHCl concentrations were made at 25 °C using an AT-105 spectrofluorimeter (Aviv Associates) and quartz cells of 0.3 × 0.3 cm cross section. The excitation wavelength was set to 297 nm (bandwidth of 1−2 nm), and the emitted fluorescence spectra were resolved to 1.0 nm after correcting for the spectral sensitivity of the spectrofluorimeter.

Time-Resolved Nonradiative Energy-Transfer Measurements. Measurements of fluorescence lifetimes were carried out by using the time-correlated single-photon counting system described previously (*2*, *3*). Fluorescence emission was collected through a polarizer oriented at the magic angle (∼55°) relative to the polarization of the exciting beam.

Decay of fluorescence emission, $I(t)$, was analyzed by nonlinear least-squares multiexponential fitting (*26*).

All measurements were made at 22 °C and pH 7.0, unless stated otherwise, with excitation at 297 nm. Two fluorescence decay curves were recorded for each set of energy-transfer experiments: (a) the fluorescence decay curve of the tryptophan residue in the absence of an acceptor in W^m-RNase A (the "D-experiment") and (b) the fluorescence decay curve of the tryptophan residue in the presence of the acceptor attached to the genetically engineered cysteine residue in the corresponding ($m-n$)-RNase A (the "DD-experiment"). The background emission was routinely subtracted from the corresponding fluorescence decay curves. To measure background emission, a solution of recombinant wt-RNase A was used. Donor emission was monitored at 360 nm (bandwidth of 12−16 nm). Data collection for each set of measurements (two samples) was carried out on the same day within a short time period. This reduced possible variations due to changes in calibration of instruments. Spectroscopic characterization of fluorescent probes, data analysis, and control experiments were described in detail in a previous study (*1*). The pair of probes used in the present study provides reliable distance determinations between 14 and 38 Å. Distances ~40 Å and higher could not be determined with high enough confidence. The fractions of the ensembles of the protein conformers which had interprobe distances of 40 Å and above are presented here despite this uncertainty because the areas under the distribution curves below 40 Å can be related to the portions of the distributions with intramolecular distances above 40 Å; thus, the fractions of molecules with distances larger than 40 Å are reasonably well represented by this analysis, despite the uncertainty.

For the cold-unfolding measurements, the temperatures were increased from 5 to 25 °C in increments of 5 °C. After reaching each target temperature, the solutions were allowed to equilibrate for 3 min. The temperatures were controlled within 0.1 °C.

RESULTS

Thermal Unfolding Transitions in Reduced RNase A. The far-UV−CD spectrum of reduced RNase A shows a very low level of secondary structure (data not shown). The 220 nm CD signal showed no sign of a thermal transition over the range of 20−80 °C (Figure 2). This result was reproducible with different reducing agents (data not shown), and it agrees with previous observations (*27*). Although reduced RNase A contains very little (or no) secondary structure, it was suggested by Navon et al. (*1*) that at least some segments of the molecule, in particular in the C-terminal subdomain which includes the hydrophobic core, are collapsed into a compact structure in the R_N state.

TR-FRET Analysis of Cold Unfolding throughout the RNase A Molecule. One aspect of the overall compactness of RNase A in the reduced state is reflected by the global cold unfolding of the molecule as determined by TR-FRET measurements, as a function of temperature. Cold unfolding was also reported previously for RNase A by Jonas and his collaborators (*28*). Figure 3 illustrates the mean intramolecular distance between the tryptophan donor and the coumarin acceptor for six segments at different temperatures measured with six different RNase A derivatives, and

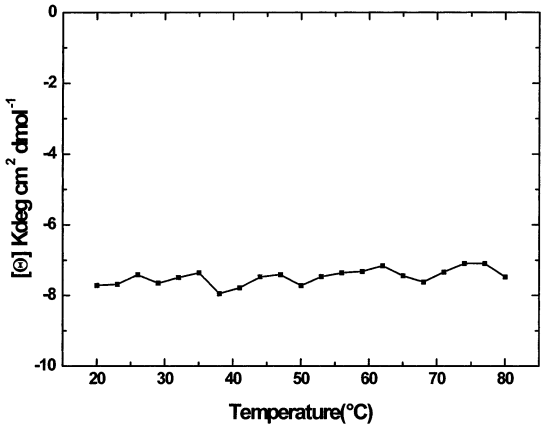

FIGURE 2: Far-UV CD (molar ellipticity) temperature transition of reduced RNase at 220 nm. RNase A was unfolded and reduced by incubation in the presence of 150 mM TCEP, 6 M GdnHCl, and 40 mM HEPES (pH 7.5) at 37 °C for 60 min. The reduced RNase A was then dialyzed against buffer containing 40 mM HEPES (pH 7.5) and 20 mM TCEP overnight. The resulting reduced RNase A (0.7 mg/mL) was used to follow the change in the CD as a function of temperature.

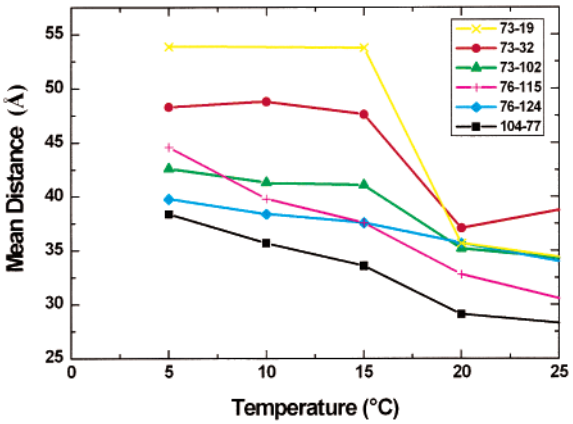

FIGURE 3: Global cold unfolding transition of different segments of the reduced RNase A mutants in the R_N state at pH 7 as a function of temperature. Mean intramolecular distance distributions were obtained from time-resolved FRET measurements at different temperatures for double-labeled ($m-n$)-RNase A mutants. The fluorescence decay of the tryptophan residue of the mutant protein was measured in 40 mM HEPES (pH 7) buffer containing 20 mM DDT and 5 mM EDTA at different temperatures (as specified for each mutant).

calculated using global analysis (*26*). Global cold unfolding, which is more pronounced for the mixed-domain segments (i.e., 73−19, 73−32), occurs below 20 °C. This global expansion of RNase A at low temperatures demonstrates that RNase A is rather compact in the reduced state and that this compactness is presumably due to local and nonlocal hydrophobic interactions, which weaken at low temperature.

Steady-State FRET Analysis of GdnHCl-Induced Denaturation Transitions. To determine whether specific segments constituting the hydrophobic core lose their compactness in a cooperative manner and whether the transitions in different segments in this region are coordinated (i.e., whether different segments in the hydrophobic core lose or assume specific structure in a hierarchic manner in the GdnHCl transition), the GdnHCl-induced unfolding/refolding transitions were monitored. These transitions were monitored by steady-state FRET detection of the long-chain segment which links the N- and C-terminal subdomains (92−32) and of several

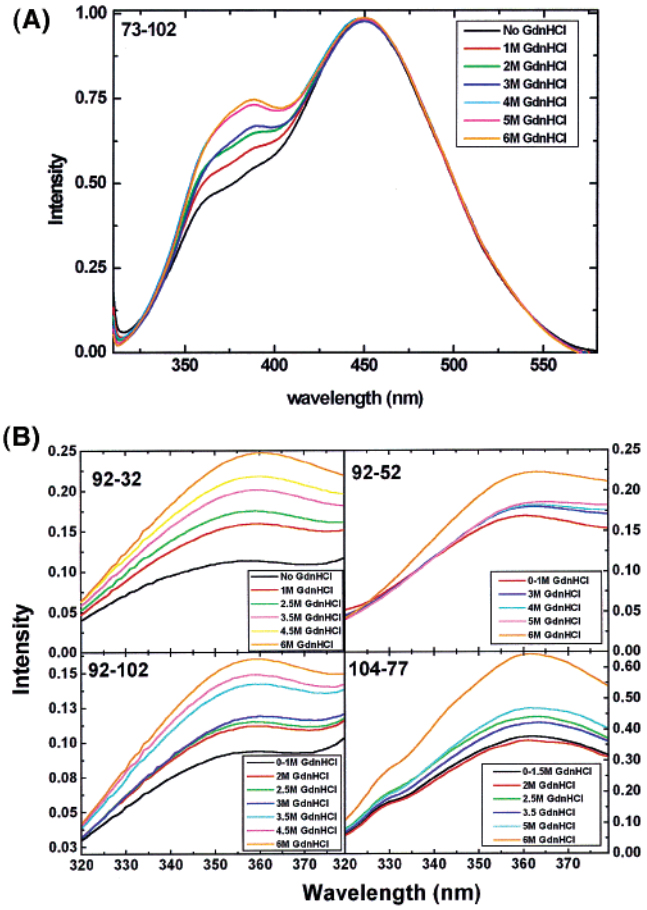

FIGURE 4: Steady-state FRET emission spectra of the donor of reduced RNase A mutants (*m*−*n*) at increasing GdnHCl concentrations at 22 °C and pH 7.0. The mutants 73−102, 92−32, 92−52, 92−102, and 104−77 (about 0.6 mg/mL) were reduced in the presence of 6 M GdnHCl, 50 mM HEPES (pH 7.0), and 150 mM DTT. Aliquots of 200 μL were dialyzed against the specified GdnHCl concentration in the presence of 20 mM DTT. The samples were filtered, and the fluorescence emission spectra were recorded with an excitation wavelength of 297 nm. The spectra were normalized at 454 nm, the emission maximum of the coumarin probe. The intensity of the donor increases as the GdnHCl concentration increases, reflecting the increased distance and reduced quenching. In (A) the results obtained for 73−102 are shown, demonstrating a typical scan. In (B) the tryptophan emission region (320−380 nm) is enlarged.

segments within the C-terminal part (73−102, 92−52, 92−102, and 104−77) of the reduced RNase A mutants. The donor emission spectra (Figure 4) show the decrease of tryptophan emission intensity relative to that of the acceptor maximal intensity (Figure 4A) upon reduction of the GdnHCl concentration. In a control experiment, we verified that the emission of the acceptor (coumarin) does not change and the fluorescence maximum does not shift when the GdnHCl concentration is changed (data not shown). This insensitivity of the acceptor spectrum to the concentration of denaturant is probably due to the location of the acceptor, which was designed to be on the surface of the molecule, and to the fact that the structures characterized for the reduced state are loosely packed. Hence, this decrease in tryptophan emission intensity is due to enhanced FRET upon reduction of the distance between the donor and excerptor. As shown in Figure 4B, the distance monitored between the N- and C-terminal subdomains (92−32) increases almost linearly as the GdnHCl concentration increases, indicating the absence of any stable intermediates. By contrast, Figure 4 shows that the changes of the donor emission intensities for several RNase mutants are nonlinear when the GdnHCl concentration is increased. Over some ranges of variation of the denaturant concentration, there are large changes in donor emission intensity, whereas there are negligible changes in other ranges of increase of the denaturant concentration. This is an indication of pronounced transitions in the conformations of the labeled chain segments in the relevant mutants. For example, the denaturation of the mutant labeled at residues 92 and 102 shows significant changes of the donor emission mainly between 1 and 2 M and between 3 and 3.5 M GdnHCl. This means that different mutants show enhanced changes of donor emission intensity at different GdnHCl concentrations. This is direct evidence for multiple conformational changes within the partially folded RNase A molecule at the subdomain level.

TR-FRET Analysis of GdnHCl-Induced Denaturation Transitions. More detailed characterization of the conformational transition of the C-terminal subdomain of several selected mutants was obtained by time-resolved FRET measurements of the GdnHCl-induced unfolding of the reduced RNase A mutants. The distributions of intramolecular distances in four labeled C-terminal chain segments, defined by the pairs of residues 76−115, 76−124, 73−102, and 104−77, were determined under various denaturant concentrations. We used only these four mutants in TR-FRET experiments because the derivatives which monitor a pair between two domains (carboxyl-terminal donor and amino-terminal acceptor), e.g. 92−32, 92−52, and 73−19, did not exhibit a distinct transition between two discrete conformations (*1*). In the pair of domains, the decrease in FRET reflects only the average change in distance between the donor and acceptor, indicating the transition between ensembles of conformations and not between defined intermediates. The mean and width of each distribution show the extent of unfolding and multiplicity of the conformations in the R_N ensemble, in response to stepwise changes of the denaturant concentrations (0 to 6 M GdnHCl) and reduction of disulfide bonds.

The intramolecular distance distributions for these four segments are shown in Figure 5. These mutants probe conformational changes in different regions of the C-terminal subdomain, presumably representing the development of loosely ordered structure in the initial formation of different parts of the hydrophobic core. When immersed in 6 M GdnHCl, the four labeled chain segments exhibited very low levels of FRET efficiency, indicating large mean end-to-end distances (>40 Å) and large widths of the distributions. These mean distances exceeded the range of reliable distance determination with the present pair of probes. (Therefore, the corresponding traces in Figure 5 do not represent the actual IDDs. Rather, they are presented here to emphasize the large intramolecular distances that exist under fully denaturing conditions.) Gradual reduction of the GdnHCl concentrations down to folding conditions (0 M GdnHCl) resulted in stepwise reduction of both the width and the mean of the distributions. This analysis of the conformational transitions in the C-terminal subdomain did not reveal a clear common cooperative transition. Instead, it showed a series of minor coordinated local transitions, probed by the different

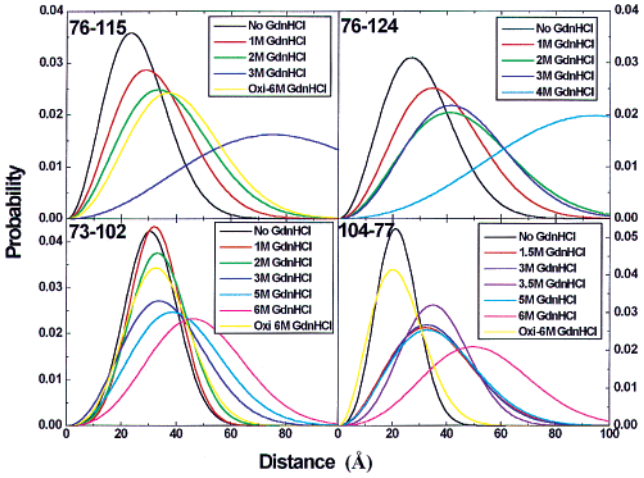

FIGURE 5: Intramolecular distance distributions from TR-FRET analysis (expressed as probabilities) at different GdnHCl concentrations, obtained for double-labeled (*m*−*n*)-RNase A mutants in the R_N and U states. The fluorescence decay of the tryptophan residue in each mutant protein was measured in 40 mM phosphate (pH 7) buffer containing 20 mM DTT and 5 mM EDTA with no GdnHCl (the R_N state) and in the presence of different concentrations of GdnHCl (as specified for each panel). The same mutants were denatured (in the presence of 6 M GdnHCl) without reduction of the disulfide bonds (the U state) (Oxi-6 M GdnHCl). (These distances include an approximately 3 Å contribution from the probes and the linker.) The experimental setup and data analysis are described in detail elsewhere (*1*).

mutants, which occurred at different concentrations of the denaturant.

Residues 104 and 77 are located at the edges of a chain segment that forms an antiparallel β structural element in the native state. Reduction of the disulfide bonds under otherwise folding conditions increased the mean distance between these two residues to 20 Å with a small width, indicative of an interaction that holds the two ends of this 28-residue segment in juxtaposition, despite the lack of evidence for the formation of the native β structure (Figure 2). This chain segment thus forms a long unstructured loop whose ends are poised for formation of a native tertiary fold. The transition toward formation of this quite dispersed structure appears to involve two distinct minor transitions, first between 6 and 5 M GdnHCl (presumably reflecting the initial compaction of the molecule) and second between 1.5 and 0 M GdnHCl (Figure 5). In Figure 5, there are three groups of distributions monitored for the 104−77 derivative: one at low GdnHCl concentration, one at GdnHCl concentration between 1.5 and 5 M, and one at 6 M GdnHCl. This means that there are two structural transitions. This result is in agreement with the previous results presented in Figure 4B, where two transitions were also monitored for mutant 104−77.

Residues 73 and 102 delineate a similar section of the chain with longer separation than that between residues 104 and 77 in the native state and correspondingly in the R_N state. This 40-residue chain segment showed the same (but smaller in magnitude) renaturation transition that was involved in 104−77. A possible cause for this lower magnitude is that the N-terminal side of this segment (residues 73−76) is not associated with the formation of the C-terminal hydrophobic nucleation cluster and is part of a flexible loop, and the transition in 73−102 will not be as sharp as that in 104−77; i.e., it is diffuse. The transition to a narrower distribution in width of the mean distances between this pair of residues **(**73−102**)**, characteristic of the R_N state, was completed between 3 and 2 M GdnHCl. The transition at the low GdnHCl end of the titration of these two chain segments reached a relatively narrow intramolecular distance distribution. This stepwise reduction of the width of the distribution is indicative of stepwise formation of a well-ordered structure.

The mutant labeled at residues 76 and 124 probes a longer chain section which, in addition to the 104−77 segment, includes the 20 C-terminal residues. This chain segment forms the C-terminal antiparallel β structure in the native state. The mean distance between residues 76 and 124 is larger than 40 Å in the denatured state at GdnHCl concentrations higher than 3 M. Only at 3 M and lower GdnHCl concentrations did the mean end-to-end distance of this chain segment reach the significant detection limit of the measurement, and it appears to have a distinct transition between 4 and 3 M GdnHCl. The 40-residue chain segment (monitored by the derivative from residue 76 to 115) includes two native-state β structure elements, the long antiparallel β sheet (residue 79 to 104) and part of the C-terminal antiparallel β structure (see Figure 1). The transition monitored by the change of the distance between residues 76 and 115 thus reflects changes in both of these structural elements. This mutant exhibits a transition between 3 and 2 M GdnHCl. Unlike the 104−77 and 73−102 mutants, the 76−115 and 76−124 mutants show much wider distributions, indicating a lower degree of order, both at high GdnHCl concentrations and in the R_N state.

The detailed analysis of the distributions of the end-to-end distances of the four chain segments revealed a complex GdnHCl-driven unfolding/refolding transition in the C-terminal subdomain of the reduced RNase A mutant molecules. At least four segmental transitions were observed in the coordinated hierarchic formation of the C-terminal structure of the reduced molecule, which is centered around the hydrophobic core: (a) a transtion between 6 and 5 M GdnHCl, which is monitored by 104−77 and 73−102, which presumably represents the initial compaction phase; (b) a transition between 4 and 3 M GdnHCl, detected here by the 76−124 pair, which presumably reflects the formation of the loop from residue 104 to 124; (c) a transition between 3 and 2 M GdnHCl, followed by 76−115, which presumably reflects formation of the loops between 79 and 104, and between 104 and 124, and interaction between them; and (d) a final transition between 1.5 and 0 M (R_N state) GdnHCl, which is detected by 104−77, 76−124, and 76−115, and probably represents the last compaction among the foregoing loops. Further support for this sequence of events is indicated by comparing the distances measured for oxidized RNase A in 6 M GdnHCl (yellow traces in Figure 5) with the distances measured between the donor and acceptor in the R_N state in these four pairs. The 58−110 disulfide bond imposes a constraint on the 104−77 and 73−102 distances in oxidized RNase A in 6 M GdnHCl, but their distances are the same as the distance measured for these two pairs in the reduce state in the absence of GdnHCl (R_N state). However, in the case of 76−124, the disulfide bonds do not impose any constraint, and, in the oxidized state in the presence of 6 M GdnHCl, the distance between this pair was too large to

monitor. In the case of 76−115, the disulfide bonds imposed constraints, and the distance measured for oxidized RNase A in 6 M GdnHCl was equal to the distance measured for reduced RNase A in the presence of 2 M GdnHCl. The effect of these different constraints indicates that the formation of disulfide bonds could occur only after the cysteines in the regions monitored here by the 104−77 and 73−102 pairs come close, while it is not necessary for the cysteines in the regions followed by 76−124 and 76−115 to achieve such close interaction.

DISCUSSION

A full understanding of the role of the initial compaction of a polypeptide chain requires the elucidation of the mechanism and kinetics of the hydrophobic collapse. In the present study, we demonstrated that the maturation of this compact state involves coordinated transitions of different chain segments of the C-terminal part of RNase A. We also succeeded in dissociating the succeeding steps, which lead to the maturation of the hydrophobic core (Figure 5). These findings were made possible through the use of nine different mutants of RNase A, each of which contained a pair of tryptophan and coumarin moieties, defining nine segments, which made it possible to follow the conformation of these nine segments independently (Figure 1) in steady-state FRET and TR-FRET experiments.

In a previous study (*1*), we demonstrated that reduced RNase A is relatively compact in the R_N state and already contains the general structural framework of the native protein. This state of the protein could be regarded as a folding intermediate which has completed the initial compaction phase and contains a developed hydrophobic core. The successive events in the folding process (i.e., to attain the fully matured secondary structures and a complete set of disulfide bonds) are presumably induced by a structural program embedded in the amino acid sequence participating in the construction of the hydrophobic core. The main goal of the present work was to characterize this collapsed state of reduced RNase A and use it as a model system to study the formation and specific transitions that promote the formation of the hydrophobic core. The rationale for the design of the present experiments was based on the notion that determination of distributions of IDDs should constitute an effective contribution in addressing major questions of interest in the context of the folding of RNase A. These include the questions of (a) whether the folding transition is a single cooperative two-state transition or a sequence of multiple subdomain transitions and (b) the extent to which formation of the native-like overall tertiary conformation of the chain segments depends on formation of secondary-structure elements, or the role that nonlocal interactions play in the initial formation of intermediate structures.

The experimental approach that combines site-directed double labeling and time-resolved FRET measurements provides a unique contribution in the present context because (a) the measurements are targeted to selected subdomain structural elements of the molecule and hence enable resolution of well-defined local transitions, and (b) the parameters obtained from the time-resolved measurements (i.e., width and mean of IDDs) are suitable for characterization of ensembles of weakly stabilized conformers.

The Compact Collapsed State of RNase A Does Not Contain Secondary Structures. The far-UV−CD experiment (Figure 2) showed very clearly that, in the R_N state of the RNase A molecule, there are very little or no secondary-structure elements. By biochemical criteria (i.e., activity, far-UV−CD), the reduced RNase A molecule could be regarded as denatured. However, in a previous study (*1*), we demonstrated that reduced RNase A is in a relatively compact state, which already contains the general structural framework of the native protein. Since the major structural framework of RNase A is based on the C-terminal antiparallel β sheets (Figure 1), it is not surprising that the R_N state is characterized by a very low amount of mature secondary structure; this is because formation of a β sheet requires interaction between pairs of residues that are separated by long-chain segments such as the 21 residues between 104 and 124, which are close to each other in space in the R_N state and in the native protein. Weak nonlocal interactions between residues close to the edges of native β elements can accelerate the formation of the native structures during the folding transitions.

The Compaction Transition Is Achieved through a Succession of Subdomain Transitions. The steady-state FRET (Figure 4) and TR-FRET experiments (Figure 5) detected thermal- and denaturant-induced segmental conformational transitions in the reduced RNase A molecule. These results confirm and further support the conclusions that (a) specific subdomain structures are weakly stabilized in the R_N state, (b) some of the segmental transitions occur under differing solution conditions **(**segments monitoring the hydrophobic core**)** and some segments showed gradual conformational change over a wide range of temperatures or GdnHCl concentrations **(**the interdomain segments**)**, and (c) the reduced RNase A molecule showed a cold unfolding (warm refolding) effect.

For several mutants, the means of the distributions of distances between pairs of residues separated by more than 20 residues (as in 104−77) were close to their crystal structure separation, despite the absence of mature secondary structure, in support of the "loop hypothesis" (*3*). According to this hypothesis, a chain segment can be unstructured while its ends are involved in a loosely stabilized interaction that keeps them in a close or native-like distance. Figures 4 and 5 show that the transitions in the chain segments of the C-terminal subdomain can reflect steps in the formation of a noncontiguous folding nucleation cluster in which the ends of two long loops are held at native-like distances (as in 104−77 and 76−124). These loops are composed of the chain segments that form the two major native antiparallel β structures (residues 79−104 and residues 106−124). When the GdnHCl concentration was reduced below 3 M, the ends of this loop assumed a native-like arrangement, as indicated by the distance measured for the 76−115 pair (Figure 5). These experiments support the view that a folding nucleus can correspond to a cluster of interacting residues, located far from each other along the sequence, and thereby bring different parts of the chain together (*3*, *29*). In particular, there are possible hydrophobic interactions between residues in the following clusters: residues 78−80, 104−107, and 116−124 (*30*, *31*). These clusters form parts of the secondary structures in the native state, yet Figure 2 shows that the nucleation does not require secondary-structure elements to

be formed in these intermediates in the R_N state. A similar conclusion was obtained from kinetic studies, which show that the kinetics does not depend on secondary structures; strong and specific hydrophobic contacts seem to play the dominant role (*32*).

These experiments further enhance the conclusion that the denatured states have a significant level of ordered structures at the tertiary level without secondary structures. In addition, these experiments emphasize the key role of the contribution of nonlocal interactions to the determination of the initial subdomain structures in the unfolded or partially folded states of the protein. A few such nonlocal native-like interactions can yield a much smaller entropy loss, with an accompanying major reduction of the available conformational space compared to the formation of a complete β sheet. These non-secondary-structure elements can then form a noncontiguous clustered folding nucleus. A combination of the present approach for determining intramolecular distance distributions with site-directed mutagenesis should be effective for identifying specific residues that contribute the interactions that lead to formation of the nucleus and control the folding mechanism.

CONCLUSIONS

Under folding conditions, reduced RNase A (R_N) shows no sign of secondary structure, yet the C-terminal domain of the molecule has a compact structure with native-like features which can undergo unfolding/refolding transitions. The results of a determination of a series of distributions of intramolecular distances are consistent with the hypothesis that a few nonlocal interactions can lead to formation of noncontiguous nuclei and very flexible loops of the chain segments. The formation of these structures during refolding is a complex combination of multiple subdomain transitions. Different structural elements of the reduced molecule undergo conformational transitions at different denaturant concentrations in a coordinated sequential manner. The early compact state of reduced RNase A is characterized by wide distributions (Figure 5) corresponding to a wide range of energies.

REFERENCES

1. Navon, A., Ittah, V., Landsman, P., Scheraga, H. A., and Haas, E. (2001) *Biochemistry 40*, 105−118.
2. Gottfried, D. S., and Haas, E. (1992) *Biochemistry 31*, 12353−12362.
3. Ittah, V., and Haas, E. (1995) *Biochemistry 34*, 4493−4506.
4. Rothwarf, D. M., Li, Y. J., and Scheraga, H. A. (1998) *Biochemistry 37*, 3760−3766.
5. Rothwarf, D. M., Li, Y. J., and Scheraga, H. A. (1998) *Biochemistry 37*, 3767−3776.
6. Iwaoka, M., Juminaga, D., and Scheraga, H. A. (1998) *Biochemistry 37*, 4490−4501.
7. Xu, X., and Scheraga, H. A. (1998) *Biochemistry 37*, 7561−7571.
8. Welker, E., Narayan, M., Volles, M. J., and Scheraga, H. A. (1999) *FEBS Lett. 460*, 477−479.
9. Wedemeyer, W. J., Welker, E., Narayan, M., and Scheraga, H. A. (2000) *Biochemistry 39*, 4207−4216.
10. Narayan, M., Welker, E., Wedemeyer, W. J., and Scheraga, H. A. (2000) *Acc. Chem. Res. 33*, 805−812.
11. Scheraga, H. A., Wedemeyer, W. J., and Welker, E. (2001) *Methods Enzymol. 341*, 189−221.
12. Welker, E., Narayan, M., Wedemeyer, W. J., and Scheraga, H. A. (2001) *Proc. Natl. Acad. Sci. U.S.A. 98*, 2312−2316.
13. Welker, E., Wedemeyer, W. J., Narayan, M., and Scheraga, H. A. (2001) *Biochemistry 40*, 9059−9064.
14. Shimotakahara, S., Rios, C. B., Laity, J. H., Zimmerman, D. E., Scheraga, H. A., and Montelione, G. T. (1997) *Biochemistry 36*, 6915−6929.
15. Laity, J. H., Lester, C. C., Shimotakahara, S., Zimmerman, D. E., Montelione, G. T., and Scheraga, H. A. (1997) *Biochemistry 36*, 12683−12699.
16. Xu, X., Rothwarf, D. M., and Scheraga, H. A. (1996) *Biochemistry 35*, 6406−6417.
17. Volles, M. J., Xu, X., and Scheraga, H. A. (1999) *Biochemistry 38*, 7284−7293.
18. Wedemeyer, W. J., Xu, X., Welker, E., and Scheraga, H. A. (2002) *Biochemistry 41*, 1483−1491.
19. Baldwin, R. L., and Rose, G. D. (1999) *Trends Biochem. Sci. 24*, 77−83.
20. Ratner, V., Kahana, E., and Haas, E. (2002) *J. Mol. Biol. 320*, 1135−1145.
21. Ghosh, A., Elber, R., and Scheraga, H. A. (2002) *Proc. Natl. Acad. Sci. U.S.A. 99*, 10394−10398.
22. Wlodawer, A., Svensson, L. A., Sjölin, L., and Gilliland, G. L. (1988) *Biochemistry 27*, 2705−2717.
23. Navon, A., Ittah, V., Laity, J. H., Scheraga, H. A., Haas, E., and Gussakovsky, E. E. (2001) *Biochemistry 40*, 93−104.
24. Woody, R. W. (1995) *Methods Enzymol. 246*, 34−71.
25. Venyaminov, S. Y., and Yang, J. T. (1996) in *Circular dichroism and the conformational analysis of biomolecules* (Fasman, G. D., Ed.) pp 69−108, Plenum Press, New York.
26. Beechem, J. M., and Haas, E. (1989) *Biophys. J. 55*, 1225−1236.
27. Noppert, A., Gast, K., Müller-Frohne, M., Zirwer, D., and Damaschun, G. (1996) *FEBS Lett. 380*, 179−182.
28. Nash, D., Lee, B. S., and Jonas, J. (1996) *Biochim. Biophys. Acta 1297*, 40−48.
29. Fersht, A. R. (2000) *Proc. Natl. Acad. Sci. U.S.A. 97*, 1525−1529.
30. Matheson, R. R., Jr., and Scheraga, H. A. (1978) *Macromolecules 11*, 819−829.
31. Montelione, G. T., and Scheraga, H. A. (1989) *Acc. Chem. Res. 22*, 70−76.
32. Oliveberg, M. (2001) *Curr. Opin. Struct. Biol. 11*, 94−100.

BI020506P